

Original Article

A QSIQR mathematical model of the Covid-19 epidemic in Indonesia
by considering government policiesMuhammad Kharis¹, Miswanto^{2*}, and Cicik Alfiniyah²¹ Program of Mathematics and Sciences, Faculty of Science and Technology,
Universitas Airlangga, Surabaya 60115, Indonesia² Department of Mathematics, Faculty of Science and Technology,
Universitas Airlangga, Surabaya, 60115 Indonesia

Received: 2 August 2024; Revised: 22 January 2025; Accepted: 7 May 2025

Abstract

COVID-19 first appeared in Wuhan, China, in late 2019. The disease quickly spread globally, causing a pandemic. This study provides an overview of the COVID-19 endemic in Indonesia through a mathematical model. One of the analysis results is the basic reproduction ratio, which is used to predict the model dynamics in the future. Based on parameter estimation and data fitting, the basic reproduction ratio is 0.184492232. Sensitivity analysis was used to determine the importance of each model parameter in the spread of the disease. The result is that the infection rate and the level of quarantine of infected people play significant roles in the dynamics of this epidemic. Next, these two parameters are defined as fuzzy membership functions using temperature as the firm number. Based on the results of the model analysis, government policy has a significant role in preventing the spread of COVID-19. This can be seen from the high infection rate, but the outbreak can subside. The novelty of this research includes quarantine for incoming populations, analysis of a model with dimensionless variables in a non-constant population, and fuzzy membership function definitions using temperature as a reference.

Keywords: COVID-19, QSIQR model, basic reproduction ratio, sensitivity analysis, fuzzy membership function

1. Introduction

COVID-19, caused by the SARS-CoV-2 virus, emerged in Wuhan City, Hubei Province, China, in December 2019, and was initially linked to a seafood market (Zhou *et al.*, 2020). Factors contributing to its rapid spread included international travel (Sharun *et al.*, 2021), limited early surveillance, delayed response efforts (Shangguan, Wang, & Sun, 2020), and community behaviors such as non-compliance with health protocols like mask-wearing, social distancing, and self-isolation (Haischer *et al.*, 2020; Muto, Yamamoto, Nagasu, Tanaka, & Wada, 2020).

On March 2nd, 2020, the Indonesian Government reported the first COVID-19 case among its citizens in DKI Jakarta (Sofian & Lestari, 2021). COVID-19 cases in Indonesia fluctuate due to factors such as government policies, public adherence to health protocols, and the emergence of virus

variants. Indonesian government responses have included social restrictions, health protocol enforcement, and mass vaccination campaigns. The effectiveness of these measures varies based on implementation, community compliance, and other factors (Roziqin, Mas'udi, & Sihidi, 2021).

Several mathematical models have been developed by researchers. Estrada (2020) has reviewed three main areas of research related to SARS-CoV-2 and COVID-19 modeling, namely: (1) epidemiology; (2) drug repurposing; and (3) vaccine development. The purpose of this review is to present the most relevant literature on virus modeling strategies so that it can help modelers navigate the ever-growing literature and find the most appropriate strategies to apply in emergencies when facing future pandemics. Ouaziz and Khomssi (2024) introduced the SEIRH where S_I is sensitive, E_I is unprotected, I is contaminated or exhibiting indications, I_{nd} denotes those who are ill but are not yet officially diagnosed, R is recuperated individuals and H is healthy persons. Kucharski *et al.* (2020) introduced the SEIT model, where T denotes transferred individuals (isolated, recovered, or no longer

*Corresponding author

Email address: miswanto@fst.unair.ac.id

infectious). Chatterjee, Chatterjee, Kumar, and Shankar (2020) explored the SEIQRD model with Quarantine (Q) and Died (D). Abdy, Side, Annas, Nur, and Sanusi (2021) devised a SIR model incorporating fuzzy parameters. Based on Chatterjee *et al.* (2020) and Abdy *et al.* (2021), we construct a mathematical model for the COVID-19 epidemic in Indonesia, incorporating government policies such as immigration quarantine, vaccination, quarantine for infected individuals, and health protocol enforcement. The novelty of this research includes quarantine for incoming populations, analysis of a model with dimensionless variables in a non-constant population, and fuzzy membership function definitions using temperature as a reference.

2. Materials and Methods

2.1 Model formulation

The transfer diagram of the model can be seen in Figure 1. The meaning of every parameter is given in Table 1. Some parameters can be controlled, like $B, \alpha, p_1, p_2, p_3,$ and p_4 .

The definition of every variable is given. $S, I,$ and R are the number of susceptible, infected, and recovered persons respectively. \bar{Q}_1 is the number of persons who enter the population and take quarantine. \bar{Q}_T is the number of quarantined infected persons. In this research, we followed Castañeda *et al.* (2023) in that the increase in new individuals (either through immigration or births) is proportional to the total population. We assumed that the birth and the natural death rates have the same value, which means that birth and natural death rates are not considered in population dynamics. In Castañeda *et al.* (2023), an analysis was conducted on a model with the birth and natural death rates having the same value but without immigration so that the resulting population dynamics are different from this study. We have also assumed the death rate because of infection of the quarantine-infected group is too small, and all immigration persons must be quarantined. Hence, $\omega = \mu, m_2 = 0,$ and $p_1 = 1,$ then based on Figure 1, we got

$$\begin{aligned} \frac{d\bar{Q}_1}{dt} &= BN - (\alpha + \mu)\bar{Q}_1 \\ \frac{d\bar{S}}{dt} &= \alpha p_2 \bar{Q}_1 + \mu N - \beta(1 - \eta p_3) \frac{\bar{S}}{N} \bar{I} - (\mu + \eta p_3) \bar{S} \\ \frac{d\bar{I}}{dt} &= \beta(1 - \eta p_3) \frac{\bar{S}}{N} \bar{I} - (\mu + m_1 + p_4) \bar{I} \\ \frac{d\bar{Q}_T}{dt} &= \alpha(1 - p_2) \bar{Q}_1 + p_4 \bar{I} - (\mu + \gamma) \bar{Q}_T \\ \frac{d\bar{R}}{dt} &= \gamma \bar{Q}_T + \eta p_3 \bar{S} - \mu \bar{R} \end{aligned} \tag{1}$$

$$N = \bar{Q}_1 + \bar{S} + \bar{I} + \bar{Q}_T + \bar{R}.$$

Then $\frac{dN}{dt} = \frac{d\bar{Q}_1}{dt} + \frac{d\bar{S}}{dt} + \frac{d\bar{I}}{dt} + \frac{d\bar{Q}_T}{dt} + \frac{d\bar{R}}{dt} = BN - m_1 \bar{I}.$

Based on the research of Mena-Lorca and Hethcote (1992), we define dimensionless variables of System (1) as follows

$$Q_1 = \frac{\bar{Q}_1}{N}, S = \frac{\bar{S}}{N}, I = \frac{\bar{I}}{N}, Q_T = \frac{\bar{Q}_T}{N}, \text{ and } R = \frac{\bar{R}}{N}.$$

$$\begin{aligned} \text{Hence } \frac{dQ_1}{dt} &= \frac{d\left(\frac{\bar{Q}_1}{N}\right)}{dt} = \frac{1}{N} \cdot \frac{d\bar{Q}_1}{dt} - \frac{\bar{Q}_1}{N} \cdot \frac{1}{N} \cdot \frac{dN}{dt} \\ &= B - (\alpha + \mu + B)Q_1 + m_1 I Q_1. \end{aligned}$$

Using a similar concept to calculate $\frac{dS}{dt}, \frac{dI}{dt}, \frac{dQ_T}{dt},$ and $\frac{dR}{dt},$ we get System (2)

$$\begin{aligned} \frac{dQ_1}{dt} &= B - (B + \mu + \alpha)Q_1 + m_1 I Q_1 \\ \frac{dS}{dt} &= \alpha p_2 Q_1 + \mu - [\beta(1 - \eta p_3) - m_1] S I - (B + \mu + \eta p_3) S \\ \frac{dI}{dt} &= \beta(1 - \eta p_3) S I - (B + \mu + m_1 + p_4) I + m_1 I^2 \\ \frac{dQ_T}{dt} &= \alpha(1 - p_2) Q_1 + p_4 I - (B + \mu + \gamma) Q_T + m_1 I Q_T \\ \frac{dR}{dt} &= \gamma Q_T + \eta p_3 S - (B + \mu) R + m_1 I R \end{aligned} \tag{2}$$

We give the initial condition of every variable in System (2) such that

$$Q_1(0) \geq 0, S(0) \geq 0, I(0) > 0, Q_T(0) \geq 0, \text{ and } R(0) \geq 0 \tag{3}$$

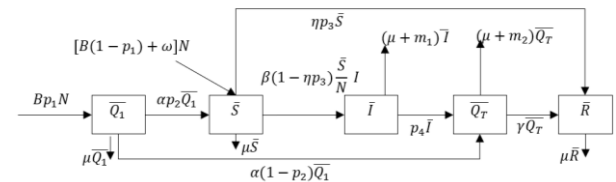


Figure 1. The transfer diagram of the QSQR mathematical model

Table 1. The definition of the parameter in the model

Parameter	Definition
B	The rate of persons entering the population from immigration
p_1	The proportion of persons quarantined from immigration
p_2	The proportion of quarantined persons free from infection
ω	The birth rate
μ	The natural death rate
p_3	The vaccination rate of susceptible persons
α	The rate of persons out of quarantine
β	The infection rate of susceptible persons
η	The effectiveness of vaccination
m_1, m_2	The death rate because of infection
p_4	The rate of infected persons who get quarantine and treatments
γ	The recovery rate of the quarantined person

2.2 Existence and boundedness of solution of the system.

Let $f = (f_1, f_2, f_3, f_4, f_5)$ where f_i is the right side of System (2) and i is the i th row, $i = 1, 2, \dots, 5$. Let $D_+^5 = \{x \in \mathbb{R}^5: x = (Q_1, S, I, Q_T, R), 0 \leq Q_1, S, I, Q_T, R \leq 1\}$. The function $f_i, i = 1, 2, \dots, 5$ has continuous first derivative then $f \in C'(D_+^5)$. Because $f \in C'(D_+^5)$ then $f: D_+^5 \rightarrow \mathbb{R}^5$ is locally Lipschitz on D_+^5 .

Proposition 1.

System (2) with initial conditions (3) has the solution in interval $[0, \infty)$ and the solution of System (2) is nonnegative for all $t \geq 0$.

Proof.

The solution of System (2) with initial conditions (3) exists on $[0, \omega)$ where $0 < \omega < \infty$ because $f = (f_1, f_2, f_3, f_4, f_5) \in C'(D_+^5)$ where f_1, f_2, \dots, f_5 are the right side of the System (2) is locally Lipschitz on D_+^5 . By using the lower bound of every equation in the System (2) (Onyango, 2022), we get

$$\begin{aligned} Q_1(t) &\geq Q_1(0)e^{-(B+\mu+\alpha)t} \geq 0 \\ S(t) &\geq S(0)e^{-\int_0^t (\beta(1-\eta p_3) - m_1 I - (B+\mu+\eta p_3)) d\tau} \geq 0 \\ I(t) &\geq I(0)e^{-(B+\mu+m_1+p_4)t} \geq 0 \\ Q_T(t) &\geq Q_T(0)e^{-(B+\mu+\gamma)t} \geq 0 \\ R(t) &\geq R(0)e^{-(B+\mu)t} \geq 0 \end{aligned}$$

with the initial conditions (3). Hence, we have completed the proof.

2.3 Parameter estimation and data fitting

System (2) was fitted to cumulative infection data in Indonesia from June 13th to November 30th, 2021, as reported by Hendratno (2022), chosen due to the outbreak's peak during this period. The quarantine duration for incoming individuals ranges from 7 to 14 days, resulting in α values between 0.07142 and 0.14286. Indonesia's total population is 270,203,917 (Badan Pusat Statistik [BPS], 2020), with an average daily immigration of 4,403.8307 persons from September 2020 to November 2021 (BPS, 2021). Parameters $\beta, p_2,$ and p_4 were estimated using the fourth-order Runge-Kutta Method, yielding $\beta = 0.97, p_2 = 0.99,$ and $p_4 = 0.9$. We also got MAPE= 0.27389122477722383 and MSE= 4.703216574231331e-09. Based on the MAPE value, the average prediction error is about 27.39% of the actual value. The very small MSE indicates that the absolute error is very small, indicating that the model is quite accurate, although the MAPE shows a relatively large percentage error. This may be due to some small actual values resulting in a high percentage error. A graphic of I data versus I estimation is given in Figure 2. The values of all parameters are given in Table 2.

2.4 Sensitivity analysis

Sensitivity analysis was carried out to determine the importance of each model parameter in the spread of disease (Marino, Hogue, Ray, & Kirschner, 2008). The sensitivity

index is used to assess the influence of each parameter on the spread of disease. The sensitivity index or Normalized sensitivity index is obtained from the normalized sensitivity index of variable V , differentiated by parameter p , defined as follows:

$$I_p^V = \frac{\partial V}{\partial p} \cdot \frac{p}{V} \tag{4}$$

where V is the variable to be analysed, and p is the parameter (Chitnis, 2005).

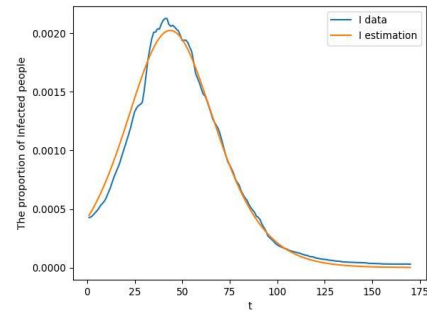


Figure 2. Plot of I data and I estimation

Table 2. The value of the parameter in the model

Parameter	Value	References
B	0.000016298	(BPS, 2020)
μ	0.0000357	(Resmawan, Nuha, & Yahya, 2021)
α	0.071428571	Assumed
m_1	0.001946408	(Hendratno, 2022)
p_2	0.99	Assumed
β	0.97	Assumed
η	0.95	(Nasir, Joyosemito, Boerman, & Ismaniah, 2021)
p_3	0.000263158	(Nasir <i>et al.</i> , 2021)
p_4	0.9	Assumed
γ	0.063065477	(Hendratno, 2022)

2.5 The membership function of the fuzzy parameter

In this research, we will define some parameters as membership functions of fuzzy parameters. Some epidemic mathematics models like Abdy *et al.* (2021), Verma, Tiwari, and Upadhyay (2018), and Nandi, Jana, Manadal, and Kar (2018) used the virus load (virus amount) as a crisp number. In this research, we will use temperature as a crisp number. Abdy *et al.* (2021) stated that the uncertain parameters or fuzzy parameters are very important because uncertainty in parameters and heterogeneity in the population are very possible to occur. Hence, the model can better describe the actual situation in the real world.

2.6 The relationship between COVID-19 and temperature

The relationship between average temperature and COVID-19 cases was nearly linear between 21°C and 30°C,

and flat beyond 21°C, with little evidence that colder weather increases infections (Abujazar, Al-Awadhi, Rachdi, & Bensmail, 2021). Weather changes significantly influence COVID-19 incidence in Jakarta, with a significant correlation found between temperatures of 26.1°C to 28.6°C and COVID-19 cases (Tosepu *et al.*, 2020). Temperatures around 26°C–

30°C with humidity over 60% do not affect COVID-19 spread (Ahmar, El Safty, Al Zahrani, Rusli, & Rahman, 2021). The optimal average temperature for COVID-19 spread is 13°C to 24°C, with cities below 24°C considered high risk for transmission (Anis, 2020). Warmer weather likely reduces COVID-19 transmissibility according to Chen *et al.* (2020).

3. Results and Discussion

3.1 The equilibrium points

The equilibrium points are determined by solving System (5).

$$\begin{aligned}
 B - (B + \mu + \alpha)Q_1 + m_1IQ_1 &= 0 \\
 \alpha p_2 Q_1 + \mu - [\beta(1 - \eta p_3) - m_1]SI - (B + \mu + \eta p_3)S &= 0 \\
 \beta(1 - \eta p_3)SI - (B + \mu + m_1 + p_4)I + m_1I^2 &= 0 \\
 \alpha(1 - p_2)Q_1 + p_4I - (B + \mu + \gamma)Q_T + m_1IQ_T &= 0 \\
 \gamma Q_T + \eta p_3 S - (B + \mu)R + m_1IR &= 0
 \end{aligned} \tag{5}$$

Theorem 2.

$$\text{Let } E_0 = (Q_1^0, S^0, I^0, Q_T^0, R^0) = \left(\frac{B}{B + \mu + \alpha}, \frac{B\alpha p_2 + (B + \mu + \alpha)\mu}{(B + \mu + \alpha)(B + \mu + \eta p_3)}, 0, \frac{B\alpha(1 - p_2)}{(B + \mu + \alpha)(B + \mu + \gamma)}, R^0 \right)$$

where $R^0 = \frac{\gamma B\alpha(1 - p_2)(B + \mu + \eta p_3) + \eta p_3[B\alpha p_2 + (B + \mu + \alpha)\mu](B + \mu + \gamma)}{(B + \mu)(B + \mu + \alpha)(B + \mu + \gamma)(B + \mu + \eta p_3)}$.

The System (2) has a disease-free equilibrium point (E_0) for every condition.

The basic reproduction ratio was determined using the next-generation matrix method (Shuai & Van Den Driessche, 2013).

Let $\mathcal{F} = \beta(1 - \eta p_3)SI$ and $\mathcal{V} = (B + \mu + m_1 + p_4)I - m_1I^2$.

$$\text{Hence, } F(E_0) = \frac{d\mathcal{F}}{dt}(E) \Big|_{E=E_0} = \beta(1 - \eta p_3)S^0 \text{ and } V(E_0) = \frac{d\mathcal{V}}{dt}(E) \Big|_{E=E_0} = (B + \mu + m_1 + p_4). \text{ We get } R_0 = \rho(FV^{-1}) = \frac{\beta(1 - \eta p_3)S^0}{B + \mu + m_1 + p_4} = \frac{\beta(1 - \eta p_3)[B\alpha p_2 + (B + \mu + \alpha)\mu]}{(B + \mu + m_1 + p_4)(B + \mu + \alpha)(B + \mu + \eta p_3)}.$$

$\rho(FV^{-1})$ means the spectral radius of matrix FV^{-1} (the maximum value of the modulus of all eigenvalues of matrix FV^{-1})

Definition 3.

$$\text{The basic reproduction ratio } (R_0) \text{ is defined } R_0 = \frac{\beta(1 - \eta p_3)[B\alpha p_2 + (B + \mu + \alpha)\mu]}{(B + \mu + m_1 + p_4)(B + \mu + \alpha)(B + \mu + \eta p_3)}.$$

Proposition 4.

1. $\beta(1 - \eta p_3) - m_1 > 0$ if $R_0 > 1$.
2. $\frac{\beta(1 - \eta p_3)[(B + \mu + \alpha) + (B + \mu + m_1 + p_4)]}{m_1[(B + \mu + \alpha) + (B + \mu + m_1 + p_4) + (B + \mu + \eta p_3)]} > 1$ if $R_0 > 1$.
3. $\frac{\beta(1 - \eta p_3)[B\alpha + (B + \mu)\mu]}{(B + \mu + \eta p_3)(B + \mu + m_1 + p_4)m_1} > 1, \frac{\beta(1 - \eta p_3)[B(B + p_4) + \mu(B + m_1 + p_4)]}{(B + \mu + \eta p_3)(B + \mu + \alpha)m_1} > 1,$
and $\frac{\beta(1 - \eta p_3)[\alpha m_1 + \mu(\alpha + m_1)]}{m_1(B + \mu + \alpha)(B + \mu + m_1 + p_4)} > 1$ if $R_0 > 1, B + \mu > m_1, B + p_4 > \alpha$.
4. $\frac{\beta(1 - \eta p_3)(\alpha + m_1 + p_4)}{m_1(B + \mu + \eta p_3 + \alpha + m_1 + p_4)} > 1$ if $R_0 > 1$.
5. $\frac{\beta(1 - \eta p_3)(\alpha + p_4)}{m_1(B + \mu + \eta p_3 + \alpha + p_4)} > 1$ if $R_0 > 1, B + \mu > m_1$ and $\alpha + p_4 > \mu$.

Proof (1).

$$\text{Let } R_{k3} = \frac{\beta(1-\eta p_3)}{m_1}.$$

$$\text{Hence } R_{k3} - R_0 = \frac{\beta(1-\eta p_3)\{(B+\mu+\alpha)[(B+\mu+p_4)(B+\mu+\eta p_3)+m_1\eta p_3]+Bm_1[B+\mu+\alpha(1-p_2)]\}}{(B+\mu+m_1+p_4)(B+\mu+\alpha)(B+\mu+\eta p_3)m_1}$$

Because $0 \leq p_2 \leq 1$ then $R_{k3} > R_0$ so $\frac{\beta(1-\eta p_3)}{m_1} > R_0$. Hence $\frac{\beta(1-\eta p_3)}{m_1} > 1$ if $R_0 > 1$.

Then $\beta(1 - \eta p_3) - m_1 > 0$ if $R_0 > 1$. The proof of numbers 2 to 5 uses similar steps.

Theorem 5.

Let $E_1 = (Q_1^*, S^*, I^*, Q_T^*, R^*)$ where

$$Q_1^* = \frac{B}{(B+\mu+\alpha)-m_1I^*}, S^* = \frac{(B+\mu+m_1+p_4)-m_1I^*}{\beta(1-\eta p_3)}, Q_T^* = \frac{B\alpha(1-p_2)+[(B+\mu+\alpha)-m_1I^*]p_4I^*}{[(B+\mu+\alpha)-m_1I^*][(B+\mu+\gamma)-m_1I^*]}$$

$R^* = \frac{\gamma Q_T^* + \eta p_3 S^*}{B+\mu-m_1I^*}$ and I^* is the solution of $g: [0,1] \rightarrow \mathbb{R}, g(I) = k_3I^3 + k_2I^2 + k_1I + k_0$ where

$$k_3 = -[\beta(1 - \eta p_3) - m_1]m_1^2,$$

$$k_2 = m_1^2[3(B + \mu) + (\alpha + m_1 + p_4 + \eta p_3)] \left[\frac{\beta(1-\eta p_3)[(B+\mu+\alpha)+(B+\mu+m_1+p_4)]}{m_1[(B+\mu+\alpha)+(B+\mu+m_1+p_4)+(B+\mu+\eta p_3)]} - 1 \right],$$

$$k_1 = -(B + \mu + \eta p_3)(B + \mu + m_1 + p_4)m_1 \left\{ \frac{\beta(1-\eta p_3)[B\alpha+(B+\mu)\mu]}{(B+\mu+\eta p_3)(B+\mu+m_1+p_4)m_1} - 1 \right\} \\ - (B + \mu + \eta p_3)(B + \mu + \alpha)m_1 \left\{ \frac{\beta(1 - \eta p_3)[B(B + p_4) + \mu(B + m_1 + p_4)]}{(B + \mu + \eta p_3)(B + \mu + \alpha)m_1} - 1 \right\} \\ - m_1(B + \mu + \alpha)(B + \mu + m_1 + p_4) \left\{ \frac{\beta(1 - \eta p_3)[\alpha m_1 + \mu(\alpha + m_1)]}{m_1(B + \mu + \alpha)(B + \mu + m_1 + p_4)} - 1 \right\} \\ - \beta(1 - \eta p_3)(Bm_1 + \alpha p_4),$$

$$k_0 = (B + \mu + \eta p_3)(B + \mu + \alpha)(B + \mu + m_1 + p_4)(R_0 - 1).$$

The System (2) has an endemic equilibrium point, i.e. $E_1 \in D_+^5$ if $R_0 > 1, B + \mu > m_1, B + p_4 > \alpha$, and $\alpha + p_4 > \mu$.

Proof. The proof is given in Appendix 1.

3.2 The local stability of equilibrium points

The Jacobian matrix of System (3) is

$$J(E) = \begin{bmatrix} J_{12} & 0 & m_1Q_1 & 0 & 0 \\ \alpha p_2 & J_{22} & J_{23} & 0 & 0 \\ 0 & \beta(1 - \eta p_3)I & J_{33} & 0 & 0 \\ \alpha(1 - p_2) & 0 & p_4 + m_1Q_T & J_{44} & 0 \\ 0 & \eta p_3 & m_1R & \gamma & J_{55} \end{bmatrix}$$

where $E = (Q_1, S, I, Q_T, R)$,

$$J_{12} = m_1I - (B + \mu + \alpha), J_{22} = -[\beta(1 - \eta p_3) - m_1]I - (B + \mu + \eta p_3),$$

$$J_{23} = -[\beta(1 - \eta p_3) - m_1]S, J_{33} = \beta(1 - \eta p_3)S - (B + \mu + m_1 + p_4) + 2m_1I,$$

$$J_{44} = m_1I - (B + \mu + \gamma), J_{55} = m_1I - (B + \mu).$$

Theorem 6.

E_0 is locally asymptotically stable if $R_0 < 1$ and E_0 is unstable if $R_0 > 1$.

Proof.

The eigenvalues of $J(E_0)$ are $\lambda_1 = -(B + \mu + \alpha), \lambda_2 = -(B + \mu + \eta p_3), \lambda_3 = -(B + \mu + \gamma), \lambda_4 = -(B + \mu)$ and $\lambda_5 = (B + \mu + m_1 + p_4)(R_0 - 1)$. We have $\lambda_1 < 0, \lambda_2 < 0, \lambda_3 < 0$, and $\lambda_4 < 0$. We get $\lambda_5 < 0$ if $R_0 < 1$ and $\lambda_5 > 0$ if $R_0 > 1$.

Hence, E_0 is locally asymptotically stable if $R_0 < 1$ and E_0 is unstable if $R_0 > 1$.

Proposition 7.

1. $\beta(1 - \eta p_3) - 2m_1 > 0$ if $R_0 > 1$ and $B + \mu > m_1$.
2. $\beta(1 - \eta p_3) - (\alpha + m_1) > 0$ if $R_0 > 1$ and $B + p_4 > \alpha$.
3. $\beta(1 - \eta p_3)p_4 - m_1(m_1 + p_4 + \eta p_3) > 0$ if $R_0 > 1$ and $p_4 > m_1$.
4. $\beta(1 - \eta p_3)(\alpha + p_4) - m_1(\alpha + p_4 + \eta p_3) > 0$ if $R_0 > 1, \alpha + p_4 > \mu$, and $B + \mu > m_1$.

The proof of proposition 7 uses similar steps as the proof of proposition 4.

Theorem 8.

E_1 is locally asymptotically stable if $R_0 > 1, B + \mu > m_1, B + p_4 > \alpha, \alpha + p_4 > \mu, p_4 > m_1, \alpha > m_1$, and $(B + p_4)(1 - p_2)\alpha > (\alpha^2 p_2 + \mu)$.

Proof. The proof is given in Appendix 2.

3.3 The global stability of equilibrium points

Theorem 9 from Shuai & Van Den Driessche (2013) provides a method to determine the Lyapunov function for the global stability of the free-disease equilibrium point.

Theorem 9. (Shuai & Van Den Driessche, 2013)

Let $f(x, y) = (F - V)x - \mathcal{F}(x, y) + \mathcal{V}(x, y)$ where $F = \left[\frac{\partial \mathcal{F}_i}{\partial x_j}(0, y_0) \right]$ and $V = \left[\frac{\partial \mathcal{V}}{\partial x_j}(0, y_0) \right]$. Let $\omega^T \geq 0$ be the left eigenvector of the nonnegative matrix $V^{-1}F$ corresponding to the eigenvalue $\rho(V^{-1}F) = \rho(FV^{-1}) = R_0$. If $f(x, y) \geq 0$ in $\Gamma \subset \mathbb{R}_+^{n+m}, F \geq 0, V^{-1} \geq 0$ and $R_0 \leq 1$ then the function $Q = \omega^T V^{-1}x$ is a Lyapunov function of model (6) in Γ .

Theorem 10.

The disease-free equilibrium point E_0 is globally asymptotically stable if $\frac{\beta(1-\eta p_3)}{(B+\mu+p_4)} \leq 1$.

Proof.

Based on Theorem 9, we get $Q = \frac{I}{B+\mu+m_1+p_4}$. Hence $Q(E_0) = 0$ and $Q(E) > 0 \forall E \in D_+^5, E \neq E_0, \dot{Q} = \frac{1}{B+\mu+m_1+p_4} \dot{I} = (R_0 - 1)I - \frac{I}{B+\mu+m_1+p_4} [\beta(1 - \eta p_3)(S^0 - S) - m_1 I]$. From the last equation, we cannot determine whether $\beta(1 - \eta p_3)(S^0 - S) - m_1 I > 0$. Hence, we change the calculation into

$$\begin{aligned} \dot{Q} &= \frac{1}{B + \mu + m_1 + p_4} \dot{I} = \frac{I}{B + \mu + m_1 + p_4} [\beta(1 - \eta p_3)S - (B + \mu + m_1 + p_4) + m_1 I] \\ &= \frac{\beta(1 - \eta p_3)I}{B + \mu + m_1 + p_4} \left[S - \frac{(B + \mu + p_4)}{\beta(1 - \eta p_3)} + m_1(I - 1) \right]. \end{aligned}$$

Hence, $\dot{Q} < 0$ if $\frac{(B+\mu+p_4)}{\beta(1-\eta p_3)} \geq 1$ or $\frac{\beta(1-\eta p_3)}{(B+\mu+p_4)} \leq 1$. Hence, the disease-free equilibrium point E_0 is globally asymptotically stable if $\frac{\beta(1-\eta p_3)}{(B+\mu+p_4)} \leq 1$.

Theorem 11.

The endemic equilibrium point E_1 is globally asymptotically stable if $R_0 > 1, p_4 = 0, B + \mu + \frac{\eta p_3}{2} \geq m_1 + \frac{\alpha p_2}{4}, B + \mu + \frac{\gamma}{2} \geq m_1 + \frac{\alpha(1-p_2)}{4}, B + \mu \geq \gamma + m_1$, and $B + \mu \geq \eta p_3 + m_1$.

Proof.

Let $V: D_+^5 \rightarrow \mathbb{R}, V(E) = \frac{1}{2} [(Q_1 - Q_1^*)^2 + (S - S^*)^2 + (Q_T - Q_T^*)^2 + (R - R^*)^2] + S^* \left(I - I^* - I^* \ln \frac{I}{I^*} \right)$ where $E = (Q_1, S, I, Q_T, R) \in D_+^5$.

We have $V(E_1) = 0$ and $V(E) > 0 \forall E \in D_+^5, E \neq E_1$.

$$\begin{aligned} \text{Hence } \dot{V} &= (Q_1 - Q_1^*)\dot{Q}_1 + (S - S^*)\dot{S} + S^*\frac{(I-I^*)}{I}\dot{I} + (Q_T - Q_T^*)\dot{Q}_T + (R - R^*)\dot{R} \\ &\leq -\alpha p_2 \left[(Q_1 - Q_1^*) - \frac{(S-S^*)}{2} \right]^2 - \left[(B + \mu + \frac{\eta p_3}{2}) - (m_1 I^* + \frac{\alpha p_2}{4}) \right] (S - S^*)^2 - \alpha(1 - p_2) \left[(Q_1 - Q_1^*) - \frac{(Q_T - Q_T^*)}{2} \right]^2 - \left[(B + \mu + \frac{\gamma}{2}) - (m_1 I^* + \frac{\alpha(1-p_2)}{4}) \right] (Q_T - Q_T^*)^2 - \frac{\gamma}{2} [(Q_T - Q_T^*) - (R - R^*)]^2 - \frac{1}{2} [(B + \mu) - (\gamma + m_1 I^*)] (R - R^*)^2 - \frac{\eta p_3}{2} [(S - S^*) - (R - R^*)]^2 - \frac{1}{2} [(B + \mu) - (\eta p_3 + m_1 I^*)] (R - R^*)^2 + p_4 (I - I^*) (Q_T - Q_T^*). \end{aligned}$$

Hence $\dot{V} < 0$ if $p_4 = 0, B + \mu + \frac{\eta p_3}{2} \geq m_1 + \frac{\alpha p_2}{4}, B + \mu + \frac{\gamma}{2} \geq m_1 + \frac{\alpha(1-p_2)}{4}, B + \mu \geq \gamma + m_1$, and $B + \mu \geq \eta p_3 + m_1$. Hence, the endemic equilibrium point E_1 is globally asymptotically stable if $R_0 > 1, p_4 = 0, B + \mu + \frac{\eta p_3}{2} \geq m_1 + \frac{\alpha p_2}{4}, B + \mu + \frac{\gamma}{2} \geq m_1 + \frac{\alpha(1-p_2)}{4}, B + \mu \geq \gamma + m_1$, and $B + \mu \geq \eta p_3 + m_1$.

3.4 Sensitivity analysis

Based on Table 2, the sensitivity index R_0 to the parameters is given in Table 3. Based on Table 3, the most sensitive parameter is β , followed by p_4, p_3 , and η . The graphs of changing parameters (by $\pm 10\%$) are given in Figure 3. The graphs of I by changing parameter η were like the graph of changing p_3 .

From Figure 3, we get that only β and p_4 have a significant influence on I . Hence, we defined the relation of both with the effectiveness of government policies. Because the range of β and p_4 is the interval $[0,1]$, we can define β and p_4 as membership functions of fuzzy parameters.

Table 3. The sensitivity index R_0 to the parameters

Parameter	The sensitivity index	Parameter	The sensitivity index
β	1	m_1	-0.002157884079
η	-0.8280701709	p_2	0.3111204437
B	0.2570642104	p_3	-0.8280701712
α	0.0002263219544	p_4	-0.9977844681
μ	0.5704719285		

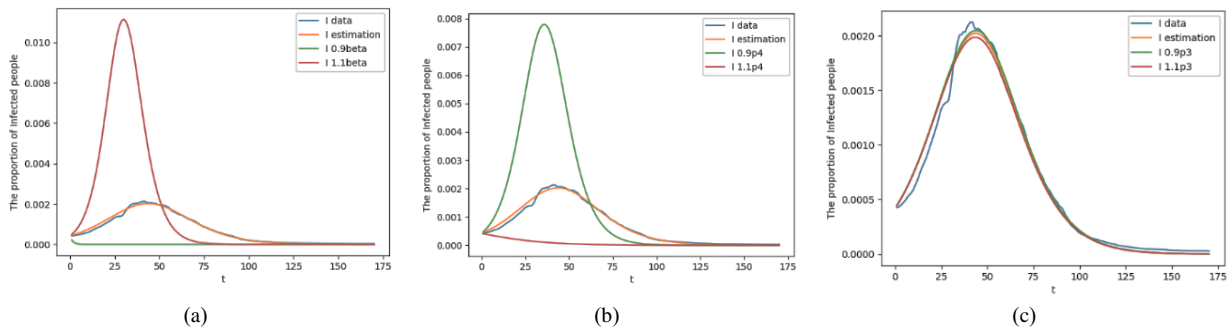


Figure 3. Plots of I on changing a parameter by $\pm 10\%$: (a) β , (b) p_4 , and (c) p_3

3.5 The membership function of the fuzzy parameter

We assumed that the humidity in Indonesia is constant. Using the membership function of the fuzzy parameter, we defined β and p_4 as follow.

$$\beta(T) = \begin{cases} \beta_{min}, & \text{if } T < T_{min} \\ \beta_{min} + \beta_1(1 - \pi)(1 - \theta) \cdot \frac{(T - T_{min})}{(T_{opt} - T_{min})}, & \text{if } T_{min} \leq T < T_{opt} \\ \beta_{min} + \beta_1(1 - \pi)(1 - \theta) \cdot \frac{(T_{max} - T)}{(T_{max} - T_{opt})}, & \text{if } T_{opt} \leq T < T_{max} \\ \beta_{min}, & \text{if } T \geq T_{max} \end{cases} \tag{6}$$

where $\beta_{min} + \beta_1(1 - \pi)(1 - \theta) = 1 \Leftrightarrow \beta_{min} = 1 - \beta_1(1 - \pi)(1 - \theta)$,

$$p_4(\beta) = \begin{cases} p_4^0, & \text{if } 0 \leq \beta < \beta_{min} \\ p_4^0 + c \cdot \beta(T), & \text{if } \beta_{min} \leq \beta < \beta(T_{opt}) \\ 1, & \text{if } \beta = \beta(T_{opt}) \end{cases}$$

and $p_4^0 + c \cdot \beta(T_{opt}) = 1 \Leftrightarrow p_4^0 = 1 - c[\beta_{min} + \beta_1(1 - \pi)(1 - \theta)]$. Hence, we get

$$p_4(T) = \begin{cases} 1 - c \cdot [\beta_{min} + \beta_1(1 - \pi)(1 - \theta)], & \text{if } T < T_{min} \\ 1 - c \cdot [\beta_{min} + \beta_1(1 - \pi)(1 - \theta)] \left[1 - \frac{(T - T_{min})}{(T_{opt} - T_{min})} \right], & \text{if } T_{min} \leq T < T_{opt} \\ 1 - c \cdot [\beta_{min} + \beta_1(1 - \pi)(1 - \theta)] \left[1 - \frac{(T_{max} - T)}{(T_{max} - T_{opt})} \right], & \text{if } T_{opt} \leq T < T_{max} \\ 1 - c \cdot [\beta_{min} + \beta_1(1 - \pi)(1 - \theta)], & \text{if } T \geq T_{max} \end{cases} \quad (7)$$

where β_1 is the standard virus transmission rate (based on the characteristics of the virus), π is the proportion of susceptible persons in implementing health protocols, θ is the effectiveness of government policies like vaccination and quarantine, and c is the weight of β for p_4 . T_{min}, T_{opt} , and T_{max} successively are minimum, optimum, and maximum temperatures ($^{\circ}C$). Let $T_{min} = 4, 13 \leq T_{opt} \leq 24$, and $T_{max} = 26$. Assume that the value of $\beta = 0.97$ and $p_4 = 0.9$ (Table 2) occurred at $T = 25, \pi = 0.8$ and $\theta = 0.698$. Then we get $c = 0.2$. The value of β, p_4 , and R_0 based on T are given in Table 4.

The graphs of I with changing temperature are given in Figure 4. From Table 4 and Figure 4, The ratio between the rate of quarantine for infected people and the rate of infection is greater, causing the outbreak to disappear more quickly.

Table 4. The value of β, p_4 , and R_0 based on T

π	θ	T	β	p_4	R_0	$\frac{p_4}{\beta}$
0.7	0.5	10	0.9505	0.9333333334	0.17434611	0.98193933
		22	1	1	0.17122169	1
		24.5	0.962875	0.95	0.17352398	0.986628586
		25	0.92575	0.9	0.17608152	0.972184715
0.8	0.698	10	0.980068	0.9333333334	0.17976964	0.952314873
		22	1	1	0.17122169	1
		24.5	0.985051	0.95	0.17752042	0.964417071
		25	0.970102	0.9	0.18451745	0.927737496

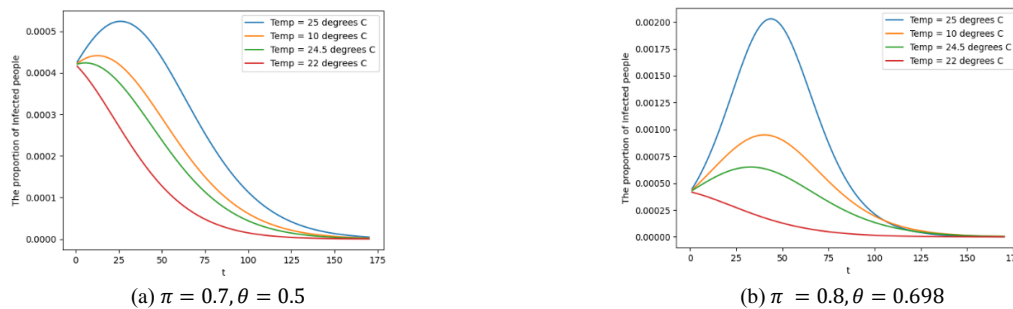


Figure 4. Plots of I for various temperatures

3.6 Numerical simulation

The initial values are given below.

$$Q_1(0) \in \{0.000017201, 0.00017201, 0.00037201\},$$

$$S(0) \in \{0.9926850995, 0.6926850995, 0.4926850995\},$$

$$I(0) \in \{0.0004196386, 0.0003196386, 0.0001196386\},$$

$$Q_T(0) = \{0.0004196386, 0.00196386, 0.00296386\}, \text{ and}$$

$$R(0) \in \{0.0064584223, 0.3048593919, 0.5038593919\}.$$

We used Table 2 for $R_0 < 1$ simulation. We got $R_0 = 0.184492232$, $E_0 = (Q_1^0, S^0, I^0, Q_T^0, R^0) = (0.000228, 0.1716, 0, 0.00000258, 0.8282)$. The simulations of $R_0 < 1$ are given in Figure 5.

From Table 2, effective countermeasures can eliminate the outbreak, indicated by $\beta = 0.97$ resulting in an R_0 value below 1. Figure 5 shows the outbreak peaked early and declined thereafter due to increasing recoveries and immunity reducing disease spread opportunities.

For global stability of the free-disease equilibrium, there is an additional condition $\frac{\beta(1-\eta p_3)}{(B+\mu+p_4)} \leq 1$ (Theorem 10). In this case, we can assign $p_3 = 0.0763158$. Hence, we got $R_0 = 0.0007124515908$, $\frac{\beta(1-\eta p_3)}{(B+\mu+p_4)} = 0.99958$, and $E_0 = (Q_1^0, S^0, I^0, Q_T^0, R^0) = (0.000228, 0.000714, 0, 0.00000258, 0.999055)$. The simulations of $R_0 < 1$ with additional condition $\frac{\beta(1-\eta p_3)}{(B+\mu+p_4)} \leq 1$ are given in Figure 5 (c) and (d). Figures 5(c) and (d) show faster convergence and the additional condition in Theorem 10 guarantees this.

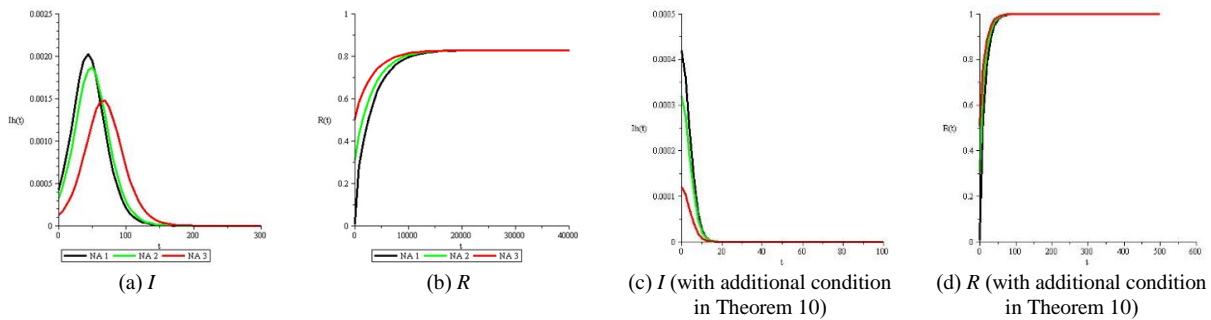


Figure 5. Simulations of $R_0 < 1$

For $R_0 > 1$, we change some parameters in Table 2, i.e., $B = 0.0036298$, $\alpha = 0.014$, $p_2 = 0.5$, $p_4 = 0$, and $\gamma = 0.000630655$. We got $R_0 = 65.053$ and all the requirements of Theorems 5, 8, and 11 are satisfied. We got that I is the solution of $k_3 I^3 + k_2 I^2 + k_1 I + k_0 = 0$ where $k_3 = -0.000003666$, $k_2 = 0.00004383$, $k_1 = -0.0000958$, and $k_0 = 0.0000248$. The cubic equation has three positive solutions i.e. 0.2994167685, 2.463945211, 9.191753991 and only one solution lies in $[0,1]$ so $I = 0.2994167685$. Hence, $E_1 = (Q_1^*, S^*, I^*, Q_T^*, R^*) = (0.212484, 0.005186, 0.299416, 0.400549, 0.082364)$. The simulations of $R_0 > 1$ are given in Figure 6.

From Figure 6, the graphs I and R converge to I^* and R^* respectively. Hence, the solution of System (2) converges to E_1 if the requirements of Theorems 5, 8, and 11 are satisfied.

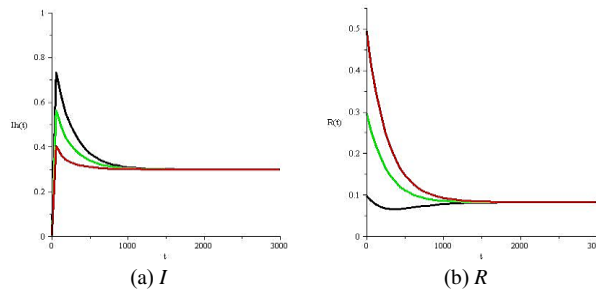


Figure 6. Simulations of $R_0 > 1$

3.7 Discussion

This study provides a new approach related to defining parameters as fuzzy membership functions with temperature as a crisp number whereas previous studies only used the virus load in the body as a crisp number such as Abdy *et al.* (2021), Nandi *et al.* (2018), and Verma *et al.* (2018). The use of temperature as a crisp number is considered more appropriate because the modelling is carried out at the macro level (individuals in a population) rather than at the cellular level. In model construction, this study is also more relevant because it pays attention to government policies such as immigration quarantine, vaccination, quarantine for infected individuals, and enforcement of health protocols, in defining the classes and parameters that play a role.

4. Conclusions

Based on data fitting using data from June 13th, 2021, to November 30th, 2021, the QSIQR model can describe the COVID-19 outbreak in Indonesia. Sensitivity analysis shows that the infection rate (β) and quarantine rate of infected people (p_4) have a significant role in the dynamics of this outbreak. Based on these results, these two parameters are then defined as a fuzzy membership functions using temperature as the crisp number and relating it to the effectiveness of government

policies and the level of community compliance in implementing health protocols. Based on the results of model analysis, the government policies have a significant role in preventing the outbreak of COVID-19. Further research that can be done includes defining fuzzy membership functions based on temperature in different parts of the region such as Tropical Zone, Subtropical Zone, Temperate Zone, and Cold Zone. Other research may divide the group of infected individuals into groups of detected infected individuals and undetected infected individuals.

Acknowledgements

This research was supported by the Education Fund Management Institution (LPDP) and Higher Education Financing Center (BPPT) from the Indonesian Education Scholarship Program (BPI) Ministry of Education, Culture, Research, and Technology (MoECRT).

References

Abdy, M., Side, S., Annas, S., Nur, W., & Sanusi, W. (2021). An SIR epidemic model for COVID-19 spread with fuzzy parameter: the case of Indonesia. *Advances in Difference Equations*, 2021(1) doi:10.1186/s13662-021-03263-6

- Abujazar, M., Al-Awadhi, S., Rachdi, M., & Bensmail, H. (2021). Effect of temperature on the spread of Covid-19 in Qatar, Kuwait and other Gulf countries. *Kuwait Journal of Science*. doi:10.48129/kjs.splcov.19499
- Ahmar, A. S., El Safty, M. A., Al Zahrani, S., Rusli, R., & Rahman, A. (2021). Association between temperature and relative humidity in relation to covid-19. *Intelligent Automation and Soft Computing*, 30(3), 795–803. doi:10.32604/iasc.2021.016868
- Anis, A. (2020). The effect of temperature upon transmission of COVID-19: australia and egypt case study. *Social Science Research Network (SSRN)*, 3567639, 1–20. doi:10.2139/ssrn.3567639
- Badan Pusat Statistik. (2020). *Jumlah Penduduk menurut Wilayah dan Jenis Kelamin, INDONESIA, Tahun 2020*. Retrieved from <https://sensus.bps.go.id/topik/tabular/sp2020/1/1/0>
- Badan Pusat Statistik. (2021). *Jumlah Kunjungan Wisatawan Mancanegara per bulan Menurut Kebangsaan (Kunjungan)*. Retrieved from <https://www.bps.go.id/id/statistics-table/2/MTQ3MCMY/jumlah-kunjungan-wisatawan-mancanegara-per-bulan-menurut-kebangsaan.html>
- Castañeda, A. R. S., Ramirez-Torres, E. E., Valdés-García, L. E., Morandera-Padrón, H. M., Yanez, D. S., Montijano, J. I., & Cabrales, L. E. B. (2023). Modified SEIR epidemic model including asymptomatic and hospitalized cases with correct demographic evolution. *Applied Mathematics and Computation*, 456. doi:10.1016/j.amc.2023.128122
- Chatterjee, K., Chatterjee, K., Kumar, A., & Shankar, S. (2020). Healthcare impact of COVID-19 epidemic in India: A stochastic mathematical model. *Medical Journal Armed Forces India*, 76(2), 147–155. doi:10.1016/j.mjafi.2020.03.022
- Chen, S., Pretner, K., Cao, B., Geldsetzer, P., Kuhn, M., Bloom, D. E., Bärnighausen, T., & Wang, C. (2020). Revisiting the association between temperature and covid-19 transmissibility across 117 countries. *In ERJ Open Research*. 6(4), 1-3. doi:10.1183/23120541.00550-2020
- Chitnis, N. R. (2005). *Using mathematical models in controlling the spread of malaria*. Tucson, AZ: The University of Arizona ProQuest Dissertations Publishing.
- Estrada, E. (2020). COVID-19 and SARS-CoV-2. Modeling the present, looking at the future. *Physics Reports*, 869, 1–51. doi:10.1016/j.physrep.2020.07.005
- Haischer, M. H., Beilfuss, R., Hart, M. R., Opielinski, L., Wrucke, D., Zirgaitis, G., . . . Hunter, S. K. (2020). Who is wearing a mask? Gender-, age-, and location-related differences during the COVID-19 pandemic. *PLoS ONE*, 15(10), 1–12. doi:10.1371/journal.pone.0240785
- Hendratno. (2022). *COVID-19 Indonesia dataset*. <https://www.kaggle.com/datasets/Hendratno/covid19-indonesia>
- Kucharski, A. J., Russell, T. W., Diamond, C., Liu, Y., Edmunds, J., Funk, S., . . . Flasche, S. (2020). Early dynamics of transmission and control of COVID-19: a mathematical modelling study. *The Lancet Infectious Diseases*, 20(5), 553–558. doi:10.1016/S1473-3099(20)30144-4
- Marino, S., Hogue, I. B., Ray, C. J., & Kirschner, D. E. (2008). A methodology for performing global uncertainty and sensitivity analysis in systems biology. *Journal of Theoretical Biology*, 254(1), 178–196. doi:10.1016/j.jtbi.2008.04.011
- Mena-Lorcat, J., & Hethcote, H. W. (1992). Dynamic models of infectious diseases as regulators of population sizes. *Journal of Mathematical Biology*, 30(7), 693–716. doi:10.1007/BF00173264
- Muto, K., Yamamoto, I., Nagasu, M., Tanaka, M., & Wada, K. (2020). Japanese citizens' behavioral changes and preparedness against COVID-19: An online survey during the early phase of the pandemic. *PLoS ONE*, 15(6), 1–18. doi:10.1371/journal.pone.0234292
- Nandi, S. K., Jana, S., Manadal, M., & Kar, T. K. (2018). Analysis of a fuzzy epidemic model with saturated treatment and disease transmission. *International Journal of Biomathematics*, 11(1). doi:10.1142/S179352451850002X
- Nasir, N. M., Joyosemito, I. S., Boerman, B., & Ismaniah, I. (2021). Kebijakan vaksinasi COVID-19: pendekatan pemodelan matematika dinamis pada efektivitas dan dampak vaksin di Indonesia [COVID-19 vaccination policy: A dynamic mathematical modeling approach to vaccine effectiveness and impact in Indonesia]. *Jurnal Pengabdian Kepada Masyarakat UBJ*, 4(2), 191–204. doi:10.31599/jabdimas.v4i2.662
- Onyango, B. A. (2022). Mathematical analysis of an Ebola model with carriers, relapse and re-infection. *Journal of Advances in Mathematics and Computer Science*, 37(9), 39–47. doi:10.9734/jamcs/2022/v37i91712
- Ouaziz, S. I., & Khomssi, M. El. (2024). Mathematical approaches to controlling COVID-19: optimal control and financial benefits. *Mathematical Modelling and Numerical Simulation with Applications*, 4(1), 1–36. doi:10.53391/mmnsa.137309
- Resmawan, Nuha, A. R., & Yahya, L. (2021). Analisis dinamik model transmisi COVID-19 dengan melibatkan intervensi karantina [Dynamic analysis of COVID-19 transmission model involving quarantine intervention]. *Jambura Journal of Mathematics*, 3(1), 66–79. doi:10.34312/jjom.v3i1.8699
- Roziqin, A., Mas'udi, S. Y. F., & Sihidi, I. T. (2021). An analysis of Indonesian government policies against COVID-19. *Public Administration and Policy*, 24(1), 92–107. doi:10.1108/PAP-08-2020-0039
- Shanguan, Z., Wang, M. Y., & Sun, W. (2020). What caused the outbreak of COVID-19 in China: From the perspective of crisis management. *International Journal of Environmental Research and Public Health*, 17(9). doi:10.3390/ijerph17093279
- Sharun, K., Tiwari, R., Natesan, S. K., Yattoo, M. I., Malik, Y. S., & Dhama, K. (2021). International travel during the COVID-19 pandemic: Implications and risks associated with “travel bubbles.” *Journal of Travel Medicine*, 27(8), 1–3. doi:10.1093/JTM/TAAA184
- Shuai, Z., & Van Den Driessche, P. (2013). Global stability of infectious disease models using Lyapunov functions. *SIAM Journal on Applied Mathematics*, 73(4), 1513–

1532. doi:10.1137/120876642

Sofian, A., & Lestari, N. (2021). Analisis framing pemberitaan tentang kebijakan pemerintah dalam menangani kasus COVID-19 [Framing analysis of news about government policies in handling COVID-19 cases]. *Commicast*, 2(1), 58. doi:10.12928/commicast.v2i1.3150

Tosepu, R., Gunawan, J., Effendy, D. S., Ahmad, L. O. A. I., Lestari, H., Bahar, H., & Asfian, P. (2020). Correlation between weather and Covid-19 pandemic in Jakarta, Indonesia. *Science of the Total Environment*, 725. doi:10.1016/j.scitotenv.2020.138436

Appendix 1. The proof of Theorem 5.

Solving equations of System (5), we get $Q_1 = Q_1^*, S = S^*, Q_T = Q_T^*$, and $R = R^*$. Hence $Q_1^* > 0, Q_T^* > 0$, and $R^* > 0$ because $B + \mu > m_1$ and $0 \leq I^* \leq 1$. Substitute the values of S^* and Q_1^* to the second equation of System (5), we got the function g where $g: [0,1] \rightarrow \mathbb{R}, g(I) = k_3 I^3 + k_2 I^2 + k_1 I + k_0$ and k_3, k_2, k_1, k_0 in Theorem 5. Based on Proposition 4, number (1) to (3), we get $k_3 < 0, k_2 > 0, k_1 < 0$, and $k_0 > 0$ if $R_0 > 1, B + \mu > m_1$, and $B + p_4 > \alpha$. Using Descartes's rule for g , we get the number of positive roots of g is either 3 or 1.

We will prove that g has only one solution in the interval $[0,1]$. We have $g(0) = k_0 > 0$ if $R_0 > 1$ and $g(1) = k_3 + k_2 + k_1 + k_0 < 0$ if $B + \mu > m_1$.

We have $g'(I) = 3k_3 I^2 + 2k_2 I + k_1$. Based on Proposition 4, we get $3k_3 < 0, 2k_2 > 0$ if $R_0 > 1$ and $k_1 < 0$ if $R_0 > 1, B + \mu > m_1$, and $B + p_4 > \alpha$.

Using Descartes's rule for g' , we get the number of positive roots of g' is either 2 or 0.

The discriminant of g' is $D = 4(k_2^2 - 3k_3 k_1)$ and $D > 0$ if $R_0 > 1$ and $(B + \mu) > m_1$. Hence, g' has two real roots.

Let

$$I_1 = \frac{2(B+\mu)}{3m_1} + \frac{1}{3} \frac{\beta(1-\eta p_3)(\alpha+m_1+p_4)-m_1(B+\mu+\eta p_3+\alpha+m_1+p_4)}{[\beta(1-\eta p_3)-m_1]m_1} + \frac{\sqrt{D}}{6[\beta(1-\eta p_3)-m_1]m_1^2}$$

Based on Proposition 4, number (4) and (5), we get $\frac{\beta(1-\eta p_3)(\alpha+m_1+p_4)-m_1(B+\mu+\eta p_3+\alpha+m_1+p_4)}{[\beta(1-\eta p_3)-m_1]m_1} > 1$ if $R_0 > 1, B + \mu > m_1$ and $\alpha + p_4 > \mu$.

$$\text{Hence, } I_1 > \frac{2}{3} + \frac{1}{3} + \frac{\sqrt{D}}{6[\beta(1-\eta p_3)-m_1]m_1^2} > 1 + \frac{\sqrt{D}}{6[\beta(1-\eta p_3)-m_1]m_1^2} > 1.$$

Hence, I_1 is an exterior point of $D_g = [0,1]$.

$$\text{Let } I_2 = \frac{-k_2 + \sqrt{D}}{3k_3} = \frac{-k_2 + \sqrt{(k_2^2 - 3k_3 k_1)}}{3k_3}$$

Because $k_3 < 0$ and $k_1 < 0$ if $R_0 > 1, (B + \mu) > m_1$, and $B + p_4 > \alpha$ then $(2k_2)^2 > (2k_2)^2 - 4(3k_3) \cdot k_1 = D$ and because $k_2 > 0$ then $-k_2 + \sqrt{D} < 0$ then $I_2 > 0$.

We get $g(I) = 3k_3(I - I_1)(I - I_2)$ if $R_0 > 1, B + \mu > m_1$, and $\alpha + p_4 > \mu$. Case $I_2 \notin [0,1]$:

We get that $I_2 > 1$ and let $I \in [0,1]$. Hence $I < I_1 \Leftrightarrow I - I_1 < 0$ and $I < I_2 \Leftrightarrow I - I_2 < 0$. Because $k_3 < 0$ then $g'(I) = 3k_3(I - I_1)(I - I_2) < 0$. Hence, g is decreasing on $[0,1]$. Because $g(0) > 0$ and $g(1) < 0$ if $R_0 > 1$ and $B + \mu > m_1$ and g continues and decreases on $[0,1]$ then $g(I) = 0$ has only one solution on $[0,1]$.

Case $I_2 \in [0,1]$:

Let $I \in [0,1]$.

Case $I \in [0, I_2]$

Hence $I < I_1 \Leftrightarrow I - I_1 < 0$ and $I < I_2 \Leftrightarrow I - I_2 < 0$. Because $k_3 < 0$ then $g'(I) = 3k_3(I - I_1)(I - I_2) < 0$. Hence, the graph of g is decreasing on $[0, I_2]$ so $g(I_2) < g(0)$.

Case $I \in [I_2, 1]$

Hence $I < I_1 \Leftrightarrow I - I_1 < 0$ and $I > I_2 \Leftrightarrow I - I_2 > 0$. Because $k_3 < 0$ then $g'(I) = 3k_3(I - I_1)(I - I_2) > 0$. Hence, the graph of g is increasing on $[I_2, 1]$ so $g(I_2) < g(1)$. Because $g(1) < 0$ then $g(I_2) < 0$.

Because $g(0) > 0$ and $g(I_2) < 0$ if $R_0 > 1$ and $B + \mu > m_1$, and g continues and decreases on $[0, I_2]$ then $g(I) = 0$ has only one solution on $[0, I_2] \subseteq [0,1]$.

Hence, the function $g: [0,1] \rightarrow \mathbb{R}, g(I) = 0$ has only one solution on the interval $[0,1]$ if $R_0 > 1, B + \mu > m_1, B + p_4 > \alpha$, and $\alpha + p_4 > \mu$.

Appendix 2. The proof of Theorem 8.

The characteristics of matrices jacobian $J(E_1)$ is

$$\begin{vmatrix} \lambda - [m_1 I^* - (B + \mu)] & [\lambda - [m_1 I^* - (B + \mu) + \gamma]](C_3 \lambda^3 + C_2 \lambda^2 + C_1 \lambda + C_0) \\ (B + \mu + \alpha) - m_1 I^* & 0 \end{vmatrix}$$

Verma, R., Tiwari, S. P., & Upadhyay, R. K. (2018). Fuzzy modeling for the spread of influenza virus and its possible control. *Computational Ecology and Software*, 8(1), 32–45.

Zhou, P., Yang, X. L., Wang, X. G., Hu, B., Zhang, L., Zhang, W., . . . Shi, Z. L. (2020). A pneumonia outbreak associated with a new coronavirus of probable bat origin. *Nature*, 579(7798), 270–273. doi:10.1038/s41586-020-2012-7

where

$$\begin{aligned} C_3 &= B + \mu + \alpha - m_1 I^*, \\ C_2 &= (B + \mu + \alpha - m_1 I^*)[(B + \mu + \alpha - m_1 I^*) + (B + \mu - m_1 I^*) + I^*[\beta(1 - \eta p_3) - m_1] + \eta p_3], \\ C_1 &= (B + \mu + \alpha - m_1 I^*)[(B + \mu + \alpha - 2m_1 I^*)[\beta(1 - \eta p_3) - m_1] I^* + (B + \mu + \eta p_3)] + (B + \mu - m_1 I^*)[\beta(1 - \eta p_3) - 2m_1] I^* + [\beta(1 - \eta p_3) - (\alpha + m_1)] m_1 I^* + [\beta(1 - \eta p_3) - m_1] p_4 I^*, \\ C_0 &= I^* [(B + \mu + \alpha - m_1 I^*)^2 [(B + \mu - m_1 I^*) \beta(1 - \eta p_3) - 2m_1] + [\beta(1 - \eta p_3) p_4 - m_1(m_1 + p_4 + \eta p_3)] + \beta(1 - \eta p_3) [B m_1 \alpha (1 - p_2 - I^*) + m_1 [B(B + \mu - m_1 I^*) + (\mu + \alpha - m_1 I^*)(B + \mu + \alpha - m_1 I^*)] (1 - I^*)]]. \end{aligned}$$

We get $\lambda_1 = -(B + \mu - m_1 I^*)$ dan $\lambda_2 = -(B + \mu + \gamma - m_1 I^*)$. Because $B + \mu > m_1$ and $I^* \in [0,1]$ then $\lambda_1 < 0$ and $\lambda_2 < 0$. We will prove that all roots of $C_3 \lambda^3 + C_2 \lambda^2 + C_1 \lambda + C_0 = 0$ have a negative real part by using Routh Hurwitz criteria, i.e., C_3, C_2, C_1, C_0 and $C_1 C_2 - C_0 C_3$ are positive.

Because $B + \mu > m_1$ and $I^* \in [0,1]$, we have $C_3 > 0$ and $C_2 > 0$.

Based on proposition 7, number (1) dan (2) then $C_1 > 0$ if $R_0 > 1, B + \mu + \alpha > 2m_1, B + \mu > m_1$, and $B + p_4 > \alpha$.

We get $C_0 > 0$ if $B + \mu > m_1, \mu + \alpha > m_1, \beta(1 - \eta p_3) > 2m_1, \beta(1 - \eta p_3) p_4 > m_1(m_1 + p_4 + \eta p_3)$, and $I^* < 1 - p_2$.

Based on proposition 7, $\beta(1 - \eta p_3) > 2m_1$ if $R_0 > 1$ and $B + \mu > m_1$ and $\beta(1 - \eta p_3) p_4 > m_1(m_1 + p_4 + \eta p_3)$ if $R_0 > 1$ and $p_4 > m_1$.

Furthermore, we must determine the conditions that must be satisfied for $I^* < 1 - p_2$.

Let I^* is a solution of $g: [0,1] \rightarrow \mathbb{R}, g(I) = k_3 I^3 + k_2 I^2 + k_1 I + k_0$ where k_3, k_2, k_1 , and k_0 are defined in Theorem 5 and $k_3 < 0, k_2 > 0, k_0 > 0$ if $R_0 > 1, k_1 < 0$ if $R_0 > 1, (B + \mu) > m_1$, and $(B + p_4) > \alpha$.

$$\begin{aligned} \text{We have } g(1 - p_2) &= k_3(1 - p_2)^3 + k_2(1 - p_2)^2 + k_1(1 - p_2) + k_0 \\ &= -[\beta(1 - \eta p_3)(B + p_4)(1 - p_2)(\alpha - m_1) + \beta(1 - \eta p_3)\mu p_2 m_1 + p_2 m_1(B + p_4)[(B + \mu) - m_1] + \beta(1 - \eta p_3)p_2(B + \mu)[(B + p_4)(1 - p_2)\alpha - (\alpha^2 p_2 + \mu)] + (B + \mu + p_4)[(B + \mu + \eta p_3) - m_1][(B + \mu + \alpha) - m_1] \\ &\quad - p_2\{\beta(1 - \eta p_3)m_1^2(1 - p_2^2) + \alpha m_1(B + \mu) + m_1[(B + \mu)(\mu + (B + \mu)) - m_1(\mu + m_1)] + m_1 \eta p_3[(B + \mu + \alpha) + (B + \mu + p_4)] + p_2^2 m_1^3 + m_1[\alpha + (B + \mu + \alpha)(B + p_2)]\} \\ &\quad - 2p_2(1 - p_2)m_1[\beta(1 - \eta p_3) - m_1][(B + p_4) - m_1] - p_2(1 - p_2)m_1[\beta(1 - \eta p_3)(\alpha + p_4) - m_1(\alpha + p_4 + \eta p_3)]. \end{aligned}$$

Based on Proposition 7 number 4, we got $\beta(1 - \eta p_3)(\alpha + p_4) - m_1(\alpha + p_4 + \eta p_3) > 0$ if $R_0 > 1, \alpha + p_4 > \mu$, and $B + \mu > m_1$. Hence, $g(1 - p_2) < 0$ if $R_0 > 1, B + \mu > m_1, \alpha + p_4 > \mu, \alpha > m_1$, and $(B + p_4)(1 - p_2) \alpha > (\alpha^2 p_2 + \mu)$.

We get $g(0) = k_0 > 0$ and $g(1 - p_2) < 0$ if $R_0 > 1, B + \mu > m_1, \alpha + p_4 > \mu, \alpha > m_1$, and $(B + p_4)(1 - p_2) \alpha > (\alpha^2 p_2 + \mu)$.

Hence, g is decreasing in the interval $[0, I_2]$ where I_2 is the least solution of $g(I) = 0$.

Cases $1 - p_2 < I_2$:

Because $g(1 - p_2) < 0, g(I^*) = 0$ and g is decreasing in interval $[0, I_2]$ then $I^* < 1 - p_2$.

Cases $1 - p_2 > I_2$:

Because $g(1 - p_2) < 0, g(I^*) = 0$ and g is decreasing in interval $[0, I_2]$ then $g(I_2) < 0$, and we get $I^* < I_2 < 1 - p_2$.

Hence, $I^* < 1 - p_2$ if $R_0 > 1, B + \mu > m_1, \alpha + p_4 > \mu, \alpha > m_1$, and $(B + p_4)(1 - p_2) \alpha > (\alpha^2 p_2 + \mu)$.

Hence, $C_0 > 0$ if $R_0 > 1, B + \mu > m_1, \alpha + p_4 > \mu, \alpha > m_1$, and $(B + p_4)(1 - p_2) \alpha > (\alpha^2 p_2 + \mu)$.

We have $C_1 C_2 - C_0 C_3 > 0$ if $B + \mu + \alpha > 2m_1$ and $B + \mu > m_1$.

Hence, the endemic point E_1 is locally asymptotically stable if $R_0 > 1, B + \mu > m_1, B + p_4 > \alpha, \alpha + p_4 > \mu, p_4 > m_1, \alpha > m_1$, and $(B + p_4)(1 - p_2) \alpha > (\alpha^2 p_2 + \mu)$.